Acta Crystallographica Section F
**Structural Biology and Crystallization Communications**
ISSN 1744-3091

# Crystallization and preliminary X-ray analysis of the *Thermoplasma acidophilum* 20S proteasome in complex with protein substrates

**Karin Felderer,[a]‡ Matthew Groves,[b] Joachim Diez,[c] Ehmke Pohl[d] and Susanne Witt[a]***

[a]Department of Molecular Structural Biology, Max-Planck Institute of Biochemistry, Am Klopferspitz 18, D-82152 Martinsried, Germany, [b]EMBL Outstation Hamburg, c/o DESY, Building 25a, Notkestrasse 85, 22603 Hamburg, Germany, [c]Paul Scherrer Institut, Swiss Light Source, CH-5232 Villigen, Switzerland, and [d]Department of Chemistry and School of Biological and Biomedical Sciences, Durham University, Durham DH1 3LE, England

‡ Present address: Department of Molecular and Cell Biology, University of California Berkeley, Berkeley, CA 94720, USA.

Correspondence e-mail: witt@biochem.mpg.de

Received 14 August 2008
Accepted 20 August 2008

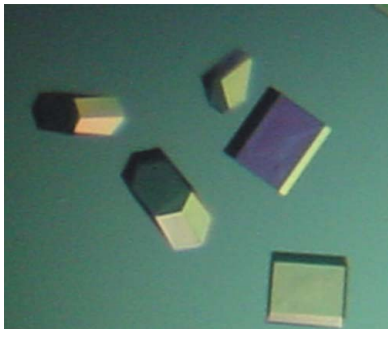



The 20S proteasome is a 700 kDa barrel-shaped proteolytic complex that is traversed by an internal channel which widens into three cavities: two antechambers and one central chamber. Entrance to the complex is restricted by the narrow opening of the channel, which only allows unfolded substrates to reach the active sites located within the central cavity. The X-ray structures of 20S proteasomes from different organisms with and without inhibitors bound have led to a detailed knowledge of their structure and proteolytic function. Nevertheless, the mechanisms that underlie substrate translocation into the 20S proteasome and the role of the antechambers remain elusive. To investigate putative changes within the proteasome that occur during substrate translocation, 'host–guest' complexes between the *Thermoplasma acidophilum* 20S proteasomes and either cytochrome *c* (cyt *c*) or green fluorescent protein (GFP) were produced and crystallized. Orthorhombic crystals belonging to space group $P2_12_12_1$, with unit-cell parameters $a = 116$, $b = 207$, $c = 310$ Å (cyt *c*) and $a = 116$, $b = 206$, $c = 310$ Å (GFP), were formed and X-ray diffraction data were collected to 3.4 Å (cyt *c*) and 3.8 Å (GFP) resolution.

## 1. Introduction

The majority of protein degradation in eukaryotic cells occurs *via* the ubiquitin–proteasome pathway. The 26S proteasome, a 2.5 MDa multisubunit molecular machine, is the key component of this pathway. In addition to its function in the degradation of misfolded and malfunctioning proteins, it plays a crucial role in controlling a variety of cellular pathways and is therefore a suitable target for anticancer drugs (Zwickl *et al.*, 1999; Glickman & Ciechanover, 2002; Goldberg, 2007). The 26S proteasome is composed of one cylindrical core particle, the ~700 kDa 20S proteasome, where proteolysis occurs and ~900 kDa 19S regulatory particles (PA700; Peters *et al.*, 1993) that can be attached to both ends of the 20S proteasome.

20S proteasomes are ubiquitous in all three kingdoms of life and their characteristic overall architecture is highly conserved (Heinemeyer *et al.*, 2004). Following the X-ray structure analysis of the archaeal 20S proteasome from *Thermoplasma acidophilum* (Löwe *et al.*, 1995), several crystal structures of 20S proteasomes from other organisms, namely the archaeon *Archaeoglobus fulgidus* (Groll *et al.*, 2003), the bacteria *Rhodococcus erythropolis* (Kwon *et al.*, 2004) and *Mycobacterium tuberculosis* (Hu *et al.*, 2006), and the eukaryote *Saccharomyces cerevisiae* (Groll *et al.*, 1997) as well as the mammalian 20S proteasome from bovine liver (Unno *et al.*, 2002), have been solved. All 20S core particles consist of 28 subunits that form a stack of four seven-membered rings ~15 nm in length and ~11 nm in diameter, with the two inner rings consisting of $\beta$-subunits sandwiched by two outer rings comprised of $\alpha$-subunits. The whole complex is traversed by a narrow central channel which widens into three cavities, a central chamber and two antechambers, that are formed at the interfaces of the four rings. The crystal structure of the 20S proteasome from *T. acidophilum* with bound acetyl-Leu-Leu-norleucinal (calpain inhibitor I) in combination with mutational studies revealed that the N-terminal threonines of the $\beta$-subunits serve as proteolytic active centres (Löwe *et al.*, 1995; Seemüller *et al.*, 1995). The 20S proteasome and other proteases that share a distinct

fold and utilise the side chain of their N-terminal residue as a nucleophile in catalytic attack are classified as N-terminal nucleophile (Ntn) hydrolases (Brannigan *et al.*, 1995).

20S proteasomes from prokaryotes are usually composed of one type of both $\alpha$-subunit and $\beta$-subunit, resulting in an $\alpha_7\beta_7\beta_7\alpha_7$ stoichiometry and 14 proteolytic active centres. Eukaryotic 20S proteasomes, however, consist of seven distinct types of both $\alpha$-subunits and $\beta$-subunits, displaying an $\alpha_{1-7}\beta_{1-7}\beta_{1-7}\alpha_{1-7}$ stoichiometry. Only three types of eukaryotic $\beta$-subunits have been shown to be active (Heinemeyer *et al.*, 1997). Despite these differences, mammalian and archaeal 20S proteasomes both degrade protein substrates into oligopeptides in a highly processive manner (Akopian *et al.*, 1997; Kisselev *et al.*, 1998, 1999).

Proteins that are destined for degradation are recognized, unfolded and translocated into the lumen of the 20S core particle by the eukaryotic 19S regulatory complexes or their archaeal analogue, the proteasome-activating nucleotidase (PAN; Voges *et al.*, 1999; Benaroudj *et al.*, 2003; Smith *et al.*, 2006). Selectivity is achieved by confining the proteolytic activity to the central chamber, which restricts access to unfolded proteins. Substrates have to wind their way through the narrow constrictions and the antechamber to reach the active sites within the central cavity. The finding that degradation by the 20S proteasome depends critically on the length of the substrate and also mathematical models indicate that not only the kinetics of proteolysis but also the translocation of substrate and product molecules determine the rate of degradation (Dolenc *et al.*, 1998; Luciani *et al.*, 2005). NMR relaxation dispersion experiments, which probe microsecond to millisecond timescale dynamics, showed that a highly dynamic environment exists inside the antechamber, which forms a surface from the entrance pore towards the catalytic chamber (Sprangers & Kay, 2007).

Although the mechanism by which proteins are degraded at the active sites has been elucidated in great detail, the mechanism underlying substrate translocation within the 20S core particle and in particular the function of the antechambers are still largely unknown.

To identify conformational changes that occur within the 20S proteasome upon substrate translocation, we attempted to crystallize 20S proteasomes from *T. acidophilum* with either cytochrome *c* (cyt *c*) or green fluorescent protein (GFP) trapped inside the inner compartments. The investigation of such 'host–guest' complexes by cryo-electron microscopy and tandem mass spectrometry revealed that several substrate molecules are sequestered within the internal cavities, thus enabling the 20S proteasome to keep substrates in store for continual degradation (Sharon *et al.*, 2006). Here, we report the crystallization and preliminary X-ray analysis of 'host–guest' complexes of the 20S proteasome.

## 2. Materials and methods

### 2.1. Expression and purification

Plasmids for the recombinant expression of 20S proteasomes were transformed into *Escherichia coli* strain BL21 (DE3). 80 l LB medium containing 100 µg ml$^{-1}$ ampicillin was inoculated with 1 l overnight culture in the same medium and the cells were grown to mid-log phase at 310 K in a large-scale fermenter. Expression was induced by adding isopropyl $\beta$-D-1-thiogalactopyranoside (IPTG) to a final concentration of 1 m*M*. Cells were harvested 8 h after induction.

$His_6$-GFP was overexpressed in *E. coli* strain KY2266 from an IPTG-inducible plasmid (pTrc99A_$His_6$-GFP). 10 l LB medium containing 50 µg ml$^{-1}$ ampicillin and 34 µg ml$^{-1}$ chloramphenicol was inoculated with an overnight culture which, in addition to ampicillin and chloramphenicol at the concentrations given above, contained 5 µg ml$^{-1}$ tetracycline. The cells were grown to mid-log phase at 303 K, expression was induced by the addition of IPTG to a final concentration of 1 m*M* and cells were harvested 18 h after induction.

For isolation of the $His_6$-tagged proteins, the bacterial pellets were resuspended in 20 m*M* sodium phosphate pH 7.4, incubated for 20 min on ice with 1 mg ml$^{-1}$ lysozyme (Sigma), a few grains of DNaseI (Roche) and one tablet per 50 ml Complete EDTA-free protease-inhibitor cocktail (Roche). Subsequently, the suspension was disrupted by three cycles at 103 MPa using an EmulsiFlex-C5 (Avestin) cell disrupter. The lysate was clarified by a low-speed spin (30 min, 4500*g*) followed by a high-speed spin (30 min, 30 000*g*). NaCl and imidazole were added to the supernatant to final concentrations of 500 and 20 m*M*, respectively. The solution was filtered through a 0.45 µm filter. Proteins were purified *via* an automated two-step purification scheme (nickel-affinity chromatography followed by gel-filtration chromatography) using an ÄKTA Explorer 10 in combination with the ÄKTA 3D kit (GE Healthcare). The system was equipped with six 1 ml HisTrap columns (GE Healthcare) and a HiLoad 16/60 Superdex 200 column (GE Healthcare). Buffer *A* containing 20 m*M* sodium phosphate pH 7.4, 500 m*M* NaCl and 20 m*M* imidazole was used as affinity binding buffer, while buffer *B* containing 20 m*M* sodium phosphate pH 7.4, 500 m*M* NaCl and 500 m*M* imidazole was used as affinity elution buffer. Size-exclusion chromatography was performed in gel-filtration buffer containing 20 m*M* HEPES pH 7.5 and 150 m*M* NaCl.

Horse-heart ferricytochrome *c* (cyt *c*) was purchased from Sigma, dissolved in gel-filtration buffer and purified on a HiLoad 16/60 Superdex 200 column (GE Healthcare) equilibrated with gel-filtration buffer.

The resulting fractions were analyzed by 12% Schaegger SDS–PAGE and fractions containing the protein of interest were pooled and concentrated for subsequent proteasome–substrate complex formation.

### 2.2. Formation of proteasome–substrate 'host–guest' complexes

'Host–guest' complexes were formed using inhibited wild-type 20S proteasome and denatured substrate molecules (cyt *c* and GFP). In the following, all concentrations are given as final concentrations in the complex-formation assay. For covalent inhibition, 1 µ*M* 20S proteasome was incubated with 70 µ*M* clasto-lactacystin-$\beta$-lactone for 30 min at room temperature. Substrates (100 µ*M*) were unfolded by incubation for 30 min at 333 K in 2.4 and 3.7 *M* guanidine–HCl when using cyt *c* and GFP as substrate, respectively. Inhibited 20S proteasomes were mixed with unfolded substrate molecules, resulting in a final concentration of 2 *M* guanidine–HCl. The solutions were incubated for 30 min (cyt *c*) and 5 min (GFP) at 333 K. For substrate refolding, the solutions were rapidly cooled on ice and incubated for 1 h on ice. When using GFP as a substrate. the solution was additionally diluted tenfold with ice-cold buffer. Complexes were separated from unbound substrate by gel-filtration chromatography on a HiLoad 16/60 Superdex 200 using gel-filtration buffer containing 20 m*M* HEPES pH 7.5 and 150 m*M* NaCl. Formation of 'host–guest' complexes was monitored using the specific spectroscopic signatures of cyt *c* at 409 nm and GFP at 395 nm and was confirmed by SDS–PAGE, Western immunoassay and electron microscopy (Sharon *et al.*, 2006). For crystallization trials, the complexes were buffer exchanged to 5 m*M* MOPS pH 7.5, 1 m*M* EDTA, 1 m*M* $NaN_3$ and concentrated to 7 mg ml$^{-1}$.

### 2.3. Crystallization

All crystallization trials were carried out using the hanging-drop vapour-diffusion method in 24-well Linbro plates (Hampton Research). 1.5 µl of a 7 mg ml$^{-1}$ solution of 'host–guest' complex in 5 m*M* MOPS pH 7.5, 1 m*M* EDTA, 1 m*M* $NaN_3$ was mixed with 0.5 µl 12%(*w*/*v*) PEG 1000, 100 m*M* potassium phosphate pH 7.5 and placed over a reservoir containing 0.5 ml 15%(*w*/*v*) PEG 1000, 100 m*M* potassium phosphate pH 7.5. Crystals grew at 293 K within one week to final dimensions of up to 0.2 × 0.3 × 0.3 mm (Fig. 1).

### 2.4. Data collection

Crystals were transferred into a cryoprotectant consisting of 12%(*w*/*v*) PEG 1000, 100 m*M* potassium phosphate pH 7.5, 30%(*v*/*v*) glycerol, scooped up in a cryoloop, mounted on the goniometer and flash-frozen in a Oxford Cryosystems Cryostream at 100 K (Teng, 1990). X-ray diffraction data were collected on a MAR CCD camera with a crystal-to-detector distance of 225 mm (cyt *c*) and 310 mm (GFP) on beamline X06SA at the SLS (Villigen) with oscillation steps of 0.2° (cyt *c*) and 1° (GFP). Diffraction images were indexed and integrated using *MOSFLM* (Leslie, 1992) and scaled with *SCALA* (Evans, 1997).

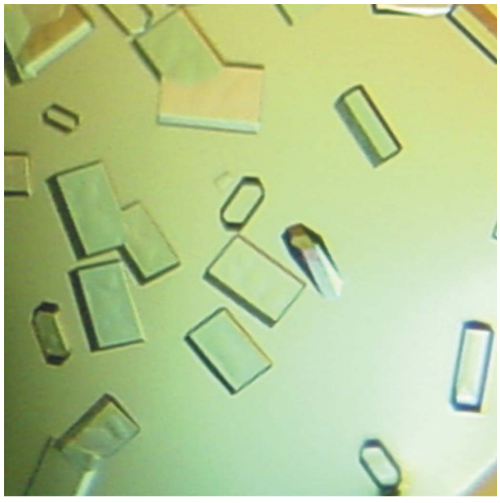

(*a*)

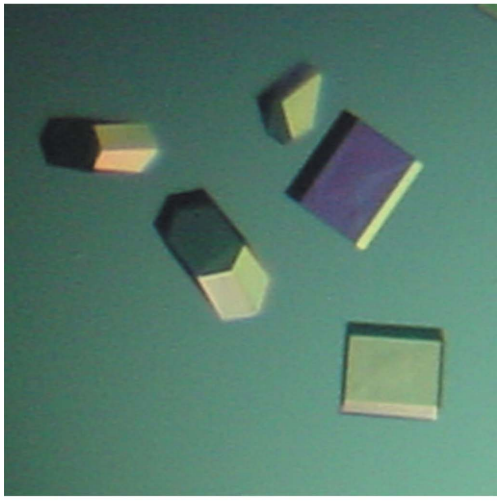

(*b*)

**Figure 1**
Crystals of 20S proteasomes in complex with (*a*) cytochrome *c* and (*b*) GFP were obtained using the hanging-drop vapour-diffusion method.

**Table 1**
Data-collection statistics.

Values in parentheses are for the highest resolution shell.

| | Cyt *c* | GFP |
|---|---|---|
| Wavelength (Å) | 0.9791 | 0.9791 |
| Space group | $P2_12_12_1$ | $P2_12_12_1$ |
| Unit-cell parameters (Å) | *a* = 116, *b* = 207, *c* = 310 | *a* = 116, *b* = 206, *c* = 310 |
| Resolution range (Å) | 50–3.35 (3.59–3.35) | 50–3.82 (4.13–3.82) |
| Total No. of reflections | 565959 (103070) | 582335 (102492) |
| No. of unique reflections | 103959 (18911) | 69886 (13844) |
| Redundancy | 5.4 (5.5) | 8.3 (7.4) |
| $R_{merge}$† | 0.127 (0.499) | 0.183 (0.547) |
| Mean $I/\sigma(I)$ | 12.6 (3.3) | 14.6 (3.6) |
| Completeness (%) | 99.6 (100.0) | 99.2 (97.7) |
| Mosaicity (°) | 0.36 | 1.2 |

† $R_{merge} = \sum_{hkl}\sum_i |I_i(hkl) - \langle I(hkl)\rangle| / \sum_{hkl}\sum_i I_i(hkl)$.

## 3. Results and discussion

Crystals of the 20S proteasome from *T. acidophilum* with either cytochrome *c* (cyt *c*) or green fluorescent protein (GFP) trapped within its internal cavities diffracted to 3.4 and 3.8 Å, respectively. Both crystals belonged to the orthorhombic space group $P2_12_12_1$, with unit-cell parameters *a* = 116, *b* = 207, *c* = 310 Å (cyt *c*) and *a* = 116, *b* = 206, *c* = 310 Å (GFP). Assuming the presence of one proteasome (28 molecules) per asymmetric unit, the Matthews coefficient is 2.9 Å$^3$ Da$^{-1}$ and the solvent content is 52.3% (Matthews, 1968). Data-collection statistics for both 'host–guest' complexes are summarized in Table 1.

Molecular-replacement calculations were performed on the 'host–guest' complexes using the structure of the native 20S proteasome from *T. acidophilum* (Löwe *et al.*, 1995; PDB code 1pma) as a model. In accordance with cryo-electron microscopy studies, the obtained electron-density map shows some additional density within the inner chambers of the complexed 20S proteasomes compared with the native structure (Sharon *et al.*, 2006). Refinement and model building are currently under way in order to reveal the conformational changes within the 20S proteasome upon substrate binding. Further mutational analysis of the residues that play a putative role in substrate translocation will provide a deeper understanding of the mechanism underlying substrate translocation into the 20S proteasome.

We would like to thank the team at the SLS for their work and support.

## References

Akopian, T. N., Kisselev, A. F. & Goldberg, A. L. (1997). *J. Biol. Chem.* **272**, 1791–1798.
Benaroudj, N., Zwickl, P., Seemuller, E., Baumeister, W. & Goldberg, A. L. (2003). *Mol. Cell*, **11**, 69–78.
Brannigan, J. A., Dodson, G., Duggleby, H. J., Moody, P. C., Smith, J. L., Tomchick, D. R. & Murzin, A. G. (1995). *Nature (London)*, **378**, 416–419.
Dolenc, I., Seemuller, E. & Baumeister, W. (1998). *FEBS Lett.* **434**, 357–361.
Evans, P. R. (1997). *Jnt CCP4/ESF–EACBM Newsl. Protein Crystallogr.* **33**, 22–24.
Glickman, M. H. & Ciechanover, A. (2002). *Physiol. Rev.* **82**, 373–428.
Goldberg, A. L. (2007). *Biochem. Soc. Trans.* **35**, 12–17.
Groll, M., Brandstetter, H., Bartunik, H., Bourenkow, G. & Huber, R. (2003). *J. Mol. Biol.* **327**, 75–83.
Groll, M., Ditzel, L., Lowe, J., Stock, D., Bochtler, M., Bartunik, H. D. & Huber, R. (1997). *Nature (London)*, **386**, 463–471.
Heinemeyer, W., Fischer, M., Krimmer, T., Stachon, U. & Wolf, D. H. (1997). *J. Biol. Chem.* **272**, 25200–25209.

Heinemeyer, W., Ramos, P. C. & Dohmen, R. J. (2004). *Cell. Mol. Life Sci.* **61**, 1562–1578.
Hu, G., Lin, G., Wang, M., Dick, L., Xu, R. M., Nathan, C. & Li, H. (2006). *Mol. Microbiol.* **59**, 1417–1428.
Kisselev, A. F., Akopian, T. N. & Goldberg, A. L. (1998). *J. Biol. Chem.* **273**, 1982–1989.
Kisselev, A. F., Akopian, T. N., Woo, K. M. & Goldberg, A. L. (1999). *J. Biol. Chem.* **274**, 3363–3371.
Kwon, Y. D., Nagy, I., Adams, P. D., Baumeister, W. & Jap, B. K. (2004). *J. Mol. Biol.* **335**, 233–245.
Leslie, A. G. W. (1992). *Jnt CCP4/ESF–EACBM Newsl. Protein Crystallogr.* **26**.
Löwe, J., Stock, D., Jap, B., Zwickl, P., Baumeister, W. & Huber, R. (1995). *Science*, **268**, 533–539.
Luciani, F., Kesmir, C., Mishto, M., Or-Guil, M. & de Boer, R. J. (2005). *Biophys. J.* **88**, 2422–2432.
Matthews, B. W. (1968). *J. Mol. Biol.* **33**, 491–497.
Peters, J. M., Cejka, Z., Harris, J. R., Kleinschmidt, J. A. & Baumeister, W. (1993). *J. Mol. Biol.* **234**, 932–937.
Seemüller, E., Lupas, A., Stock, D., Löwe, J., Huber, R. & Baumeister, W. (1995). *Science*, **268**, 579–582.
Sharon, M., Witt, S., Felderer, K., Rockel, B., Baumeister, W. & Robinson, C. V. (2006). *J. Biol. Chem.* **281**, 9569–9575.
Smith, D. M., Benaroudj, N. & Goldberg, A. (2006). *J. Struct. Biol.* **156**, 72–83.
Sprangers, R. & Kay, L. E. (2007). *Nature (London)*, **445**, 618–622.
Teng, T.-Y. (1990). *J. Appl. Cryst.* **23**, 387–391.
Unno, M., Mizushima, T., Morimoto, Y., Tomisugi, Y., Tanaka, K., Yasuoka, N. & Tsukihara, T. (2002). *Structure*, **10**, 609–618.
Voges, D., Zwickl, P. & Baumeister, W. (1999). *Annu. Rev. Biochem.* **68**, 1015–1068.
Zwickl, P., Voges, D. & Baumeister, W. (1999). *Philos. Trans. R. Soc. Lond. B Biol. Sci.* **354**, 1501–1511.